VOL. 17, NO. 10, MAY 2022 ISSN 1819-6608
ARPN Journal of Engineering and Applied Sciences

www.arpnjournals.com

MHD FREE CONVECTION AND THE EFFECTS OF SECOND ORDER CHEMICAL REACTIONS AND DOUBLE STRATIFICATION JEFFREY FLOW THROUGH POROUS MEDIUM OVER AN EXPONENTIALLY STRETCHING SHEET

B. Reddappa[1], M. Sudheer Babu[1] and S. Sreenadh[2]
[1]Department of BS and H, Sree Vidyanikethan Engineering College, Tirupati, Andhra Pradesh, India
[2]Department of Mathematics, Sri Venkateswara University, Tirupati, Andhra Pradesh, India
E-Mail: drbreddappa@gmail.com

ABSTRACT

The goal of this research was to apply the characteristics of a second-order chemical reaction to a constant flow of MHD Jeffrey fluid through an electrically conducting stratified porous media across an exponentially stretched sheet. The BVP4c approach and the sequential application of the associated similarity variables yield the PDE numerical solution that controls flow. The charts show exhaustively the results of impartial effects on energy, temperature, and liquid fixation. The coefficient of rubbing, pace of hotness move, and mass exchange coefficients are totally portrayed and measured. A benchmark comparison benchmark is used to assess the veracity of the generated findings.

Keywords: chemical reaction; MHD; stretching sheet; jeffrey flow; porous medium.

1. INTRODUCTION

Extrusion processes rely heavily on fluid dynamics induced by stretching sheets. Non-Newtonian fluids have significantly improved, according to recent research. This expansion may be tracked using a specific type of liquid used in a variety of technical and industrial applications such as compound sheet industries, glass blasting, paper making, and mechanics extrusion of plastic sheets. The vehicle of liquid over an extending surface is being contemplated by various scholastics [1-5]. Hotness move across a dramatically expanding ceaseless surface with pull was given another aspect by Elbashbeshy [6]. Ali [7] investigated the thermal boundary layer in the law of force by absorbing or injecting into a continuous stretch. Vajravelu and Cannon [9], as well as Vajravelu and Vajravelu [8], studied the flow across an indirect elastic sheet. Khan [10], Sanjayan and Khan [11], as well as others, have looked into the flow of viscous-elastic physical phenomena and, as a result, the heat transfer generated by the elastic sheet. The impact of heat radiation on physical phenomena as a result of the expandable sheet was later investigated by Sajid and Hayat [12] using the homotopy analysis technique.

An incredible number of mathematicians are keen on temperamental MHD stream across an upward permeable plate with second-request substance response. There has been a great deal of investigation into the effect of mass exchange in Newtonian and Non-Newtonian liquids lately. Nadeem et al. explored the impacts of warm radiation on nano-liquid to an adaptable sheet with convective limit conditions [13]. Chemical engineering, electrochemistry, and polymer manufacturing all benefit from the flow of MHD across a large area [14]. A portion of the jobs in the MHD stream have been recognized in the writing [15-17]. Kharabela *et al*. [18] concentrated on MHD nanofluid stream with smooth limit conditions and extraordinary compound collaborations. The impact of compound response request and convective stream with heat radiation and limit conditions on micropolar liquid across an extending sheet was explored by Matta and Gajjela [19]. Usman *et al*. [20] investigated MHD free convective synthetic response impacts within the sight of fluctuating pull.

The absorption/spraying process has ramifications for a variety of technical activities, including thrust bearing and radial diffuser design, as well as thermal oil recovery [21]. Chemical reactions use absorption to eliminate reactants [22]. Mukhopadhyay [23] explored the impacts of slip, attractions, and blowing on a precarious blended convection stream past an extending sheet.

Temperature differences, concentrations, or fluids with differing densities cause stratification in the flow phase. Because of its relevance in modifying transport conditions, the impacts of stratification are significant in investigating the flow of the boundary layer. [24] The movement of the MHD boundary layer to the thermal stratified area was investigated. Sekhar [25] explored limit layer occasions and hotness transmission in a thermally defined climate and found that warm partition speeds up heat move at the top. In MHD free convection in micropolar liquid, Singh and Kumar [26] investigated the event of twofold delineation, synthetic responses, heat creation, and ohmic warming.

In different specialized and modern applications, open media stream is utilized in MHD stream meters, MHD siphons, and MHD power generators [27, 28]. Furthermore, the polymer area will offer a wide scope of utilizations for explicit stream in extending sheets. Anwar *et al*. what's more, Cortell *et al*. explored the gooey leading liquid streaming around the expandable sheet with a consistent level of extending following [29, 30]. Sharma *et al*. [31] scrutinized the impact of compound cycles and ohmic scattering in a positive climate, and Pattnaik *et al*. [32] investigated MHD flow by regular sucking / injection into the pore area. Kim and Vafai [33] and Liao and Pop

[34] provide detailed descriptions of the horizontal layers flowing across the vertical plate immersed in the hollow. Tripathy *et al.* [35] utilized a permeable medium to research the impact of synthetic cycles on the free convective MHD surface over a straight flight way. Nagur Meeraiah *et al.* [36] investigated unsteady MHD boundary layer flow and heat transfer of a casson fluid past a stretching sheet.

The objective of this review is to analyze a numerical model for constant MHD limit layer stream of a Jeffrey liquid through a dramatically porous extending sheet with second-request compound response and twofold separation, which was motivated by past research. The overseeing conditions (PDEs) are changed over into ODEs and afterward settled utilizing MATLAB bvp4c. The effects of different predominant stream speed, temperature, and focus profile factors have been portrayed in charts and tables.

2. FLOW MODEL CONFIGURATION

The flow of the electromagnetic boundary layer with both sides of the viscous liquid in an explicit area in the middle of the perforated area is considered in this study. Accept the surface region is stretched out with energy $\tilde{U}$ through $\tilde{y}$ - the normal axis and the $\tilde{x}$ - axis on it. A flexible magnet field $B = B_0 e^{\frac{\tilde{x}}{2L}}$ is implemented normal to the surface and B_0 is constant. Temperature difference is developed by maintaining surface at temperature $\tilde{T}_w(x)$, which is superior to the $\tilde{T}_\infty$ (constant temperature) of the surrounding fluid and concentration $\tilde{C}_w(x)$ is more prominent than the $\tilde{C}_\infty$ (constant concentration). Taken $\tilde{T}_w(x) = \tilde{T}_0 + be^{\frac{\tilde{x}}{2L}}$, $\tilde{T}_\infty(x) = \tilde{T}_0 + ce^{\frac{\tilde{x}}{2L}}$, $\tilde{C}_w(x) = \tilde{C}_0 + me^{\frac{\tilde{x}}{2L}}$ and $\tilde{C}_\infty(x) = \tilde{C}_0 + ne^{\frac{\tilde{x}}{2L}}$ where reference temperature $\tilde{T}_0$, reference concentration $\tilde{C}_0$ and b, c, m, n are greater than zero.

The equations that regulate fluid flow are as ensues:

$$\frac{\partial \tilde{u}}{\partial \tilde{x}} + \frac{\partial \tilde{v}}{\partial \tilde{y}} = 0 \tag{1}$$

$$\tilde{u}\frac{\partial \tilde{u}}{\partial \tilde{x}} + \tilde{v}\frac{\partial \tilde{v}}{\partial \tilde{y}} = \frac{\upsilon}{1+\lambda_1}\frac{\partial^2 \tilde{u}}{\partial \tilde{y}^2} - \frac{\sigma B^2}{\rho}\tilde{u} - \frac{\upsilon}{K'(1+\lambda_1)}\tilde{u} \tag{2}$$

$$\tilde{u}\frac{\partial \tilde{T}}{\partial \tilde{x}} + \tilde{v}\frac{\partial \tilde{T}}{\partial \tilde{y}} = \alpha\frac{\partial^2 \tilde{T}}{\partial \tilde{y}^2} - \frac{1}{\rho c_p}\left(\tilde{T} - \tilde{T}_\infty\right) - \frac{\upsilon}{c_p(1+\lambda_1)}\left(\frac{\partial \tilde{u}}{\partial \tilde{y}}\right)^2 \tag{3}$$

$$\tilde{u}\frac{\partial \tilde{C}}{\partial \tilde{x}} + \tilde{v}\frac{\partial \tilde{C}}{\partial \tilde{y}} = D\frac{\partial^2 \tilde{C}}{\partial \tilde{y}^2} - k_r\left(\tilde{C} - \tilde{C}_\infty\right)^2 \tag{4}$$

where $\tilde{u}$ and $\tilde{v}$ are the components of velocity in the $\tilde{x}$ and $\tilde{y}$ directions respectively, $\tilde{T}$ is the fluid temperature, $K' = k^* e^{-\frac{\tilde{x}}{L}}$ is the permeability (k^* is constant), the variable rate of chemical conversion of the second- order irreversible reaction is the form of $k_r = \frac{1}{2}\left(\frac{k_0}{m}\right)e^{\frac{\tilde{x}}{2L}}$ where k_0 is a constant.

Within the confines of the boundary conditions:

$$\tilde{u} = \tilde{U} = \tilde{U}_0 e^{\frac{\tilde{x}}{L}},\ \tilde{v} = -\tilde{V}(\tilde{x}) = -\tilde{V}_0 e^{\frac{\tilde{x}}{L}},$$
$$\tilde{T} = \tilde{T}_w(\tilde{x}) = \tilde{T}_0 + be^{\frac{\tilde{x}}{2L}},\ \tilde{C} = \tilde{C}_w(\tilde{x}) = \tilde{C}_0 + me^{\frac{\tilde{x}}{2L}}$$
at $\tilde{y} = 0$ (5)

$$\tilde{u} \to 0,\ \tilde{T} = \tilde{T}_\infty(\tilde{x}) = \tilde{T}_0 + ce^{\frac{\tilde{x}}{2L}},\ \tilde{C} = \tilde{C}_\infty(\tilde{x}) = \tilde{C}_0 + ne^{\frac{\tilde{x}}{2L}} \text{ as } \tilde{y} \to \infty \tag{6}$$

here $\tilde{U}_0$ is reference velocity, $\tilde{V}(\tilde{x}) > 0$ is velocity of suction and $\tilde{V}(\tilde{x}) < 0$ is velocity of blowing. $\tilde{V}_0 > 0$ is the initial strength of suction and $\tilde{V}_0 < 0$ is the initial strength of blowing.

$$\eta = \sqrt{\frac{\tilde{U}_0}{2\upsilon L}}e^{\frac{\tilde{x}}{2L}}\tilde{y},\quad \tilde{u} = \tilde{U}_0 e^{\frac{\tilde{x}}{L}} f'(\eta),$$
$$v = -\sqrt{\frac{\upsilon \tilde{U}_0}{2L}}e^{\frac{\tilde{x}}{2L}}\left\{f(\eta) + \eta f'(\eta)\right\},\quad \theta(\eta) = \frac{T - T_\infty}{T_w - T_0} \text{ and}$$
$$\phi(\eta) = \frac{C - C_\infty}{C_w - C_0} \tag{7}$$

The governing equations change when (7) is substituted into equations (2), (3), and (4).

$$f''' + (1+\lambda_1) f f'' - 2(1+\lambda_1) f'^2 - K f' - M(1+\lambda_1) f' = 0 \tag{8}$$

$$(1+\lambda_1)\left(1+\frac{4R}{3}\right)\theta'' + \Pr(1+\lambda_1)\begin{pmatrix} f\theta' - f'\theta \\ -St\, f' + Q_H\,\theta \end{pmatrix} + \Pr Ec\, f''^2 = 0 \tag{9}$$

$$\phi'' + Sc\left(f\phi' - f'\phi - (St_1) f' - Cr\,\phi^2\right) = 0 \tag{10}$$

The transformed boundary conditions take the following form:

$$f' = 1,\ f = S,\ \theta = 1 - St,\ \phi = 1 - St_1 \text{ at } \eta = 0 \tag{11}$$

$$f' \to 0,\ \theta \to 0,\ \phi \to 0 \text{ as } \eta \to \infty \tag{12}$$

where $K=\frac{2L\upsilon}{k*U_0}$-Porosity parameter, $M=\frac{2\sigma B_0^2 L}{\rho U_0}$-Magnetic parameter, $\Pr=\frac{\upsilon}{\alpha}$- Prandtl number, $Q_H=\frac{2LQ_0}{U_0\rho c_p}$- Heat source parameter, $St=\frac{c}{b}$- Thermal stratified parameter, $Sc=\frac{\upsilon}{D}$- Schmidt number, $St_1=\frac{n}{m}$- Chemically stratified parameter, $Cr=\frac{k_0 L}{U_0}$- Rate of reaction parameter, $S=\frac{V_0}{\sqrt{\frac{\upsilon U_0}{2L}}}$- Suction parameter, respectively. $S<0$ is blowing and $S>0$ is suction parameters.

The important physical quantities of interest are the skin fiction coefficient C_f, local Nusselt number Nu and local Sherwood number Sh defined as:

$$C_f=\frac{\tilde{\tau}_w}{\rho\tilde{U}^2/2},\ Nu=\frac{\tilde{x}\tilde{q}_w}{k\left(\tilde{T}_w-\tilde{T}_\infty\right)},\ Sh=\frac{\tilde{x}\tilde{J}_w}{D\left(\tilde{C}_w-\tilde{C}_\infty\right)} \quad (13)$$

where $\tilde{\tau}_w$, $\tilde{J}_w$ and $\tilde{q}_w$ are the shear stress, mass flux and heat flux at the surface, respectively and are determined as

$$\tilde{\tau}_w=\mu\left(\frac{\partial\tilde{u}}{\partial\tilde{y}}\right)_{\tilde{y}=0},\quad \tilde{q}_w=-k\left(\frac{\partial\tilde{T}}{\partial\tilde{y}}\right)_{\tilde{y}=0},\ \tilde{J}_w=-D\left(\frac{\partial\tilde{C}}{\partial\tilde{y}}\right)_{\tilde{y}=0} \quad (14)$$

The dimensionless skin friction coefficient, mass transfer rate and wall heats are calculated using equation (7):

$$f''(0)=\frac{C_f}{\sqrt{\frac{2}{\mathrm{Re}}}\sqrt{\frac{\tilde{x}}{L}}},\ -\theta'(0)=\frac{Nu(1-St)}{\sqrt{\frac{\tilde{x}}{L}}\sqrt{\frac{\mathrm{Re}}{2}}} \text{ and}$$
$$-\phi'(0)=\frac{Sh(1-St)}{\sqrt{\frac{\mathrm{Re}}{2}}\sqrt{\frac{\tilde{x}}{L}}} \quad (15)$$

where the local Reynolds number $\mathrm{Re}=\frac{\tilde{U}\tilde{x}}{\upsilon}$.

3. NUMERICAL METHOD

Adding more variables to convert higher order differential equations to linear differential equations. $f_1=f,\ f_2=f',\ f_3=f'',\ f_4=\theta,\ f_5=\theta',\ f_6=\phi,\ f_7=\phi'$

Equations (8)–(10) are transformed into the following the first order ODE.

$$f_2'=f_3,\ f_3'=-(1+\lambda_1)f_1f_3+2(1+\lambda_1)f_2^2+Kf_2+M(1+\lambda_1)f_2$$
$$f_4'=f_5,\ f_5'=\left(\frac{-3\Pr}{3+(4R)}\right)\left[f_1f_5-f_2f_4-St\,f_2+Q_Hf_4\right]-\left(\frac{3\Pr Ec}{(1+\lambda_1)(3+(4R)}\right)f_3^2$$
$$f_6'=f_7,\ f_7'=(-Sc)\left[f_1f_7-f_2f_6-(St_1)f_2-Cr\,f_6^2\right]$$

To show the physical relevance of non-dimensional parameters, the approximate solutions are numerically derived using MATLAB bvp4c programming.

4. RESULTS AND DISCUSSIONS

Mathematical reproductions for different stream boundaries in pressure, warm limit layers, fixation and friction factor coefficient, Nusselt region number, and Sherwood region number were performed utilizing the methodology laid out in the first segment to look at the discoveries. Graphs and tables are used. Non-dimensional parameter values are chosen in arithmetic as $\lambda_1=0.5,\ M=1.5,\ S=0.1,\ R=0.2,\ St=0.1,\ \Pr=1.0,$ $Ec=0.2, St_1=0.1, K=1.0, Q_H=0.2, Sc=0.4, Cr=0.5$ which remain unchanged throughout the current simulation.

The impacts of Jeffrey boundary λ_1 on force, hotness, and fixation profiles are portrayed in Figures 1, 2, and 3. Obviously, when λ_1 builds, the speed profile deteriorates, and the slimness of the limit layer decays (Figure-1). It is obvious from Figures 2 and 3 that as the worth of λ_1 increments, so does the temperature and focus profile. Figures 4, 5, and 6 show the impact of the porosity boundary K on speed, temperature, and fixation field. Clearly expanding the worth of K diminishes the energy stream rate (Figure-4). The existence of a porous media imposes extra constraints on fluid flow, lowering flow and, as a result, lowering momentum. Figures 5 and 6 show how increasing K values enhances heat and concentration curves. The reason for Figures 7, 8, and 9 is to explore the effect of attractive boundary M on energy, temperature, and fixation bends. It has been found that as energy builds, the relating limit layer thickness diminishes because of an expansion in the M. (Figure-7). The presence of Lorentz energy causes transport opposition, and the stream rate diminishes as the temperature rises. Liquid stream is slow, and energy is lost underneath the limit layer. The thickness of both the warm and fixation limit layers increments when the attractive boundary increments, as displayed in Figures 8 and 9. Figure-10 portrays temperature profiles in the limit layer for pull and blowing for different upsides of the warm radiation boundary R. It may be deduced from this that increasing thermal radiation improves heat transmission. The thermal boundary layer thickness decreases as the Prandtl number $\Pr$ grows, as shown in Figure-11. Thermal conductivity is

lowered in high Pr fluids, and thermal boundary layer structures are thinner. As Pr grows, the temperature of the fluid lowers as the rate of heat transmission increases. The temperature drops as the thermal stratification parameter St is increased, as shown in Figure-12. The rising temperature profiles with increasing heat source parameter Q_H are depicted in Figure-13. The influence of Eckert number Ec on the temperature profile is shown in Figure 14. It has been observed that as Ec rises, so does temperature. The fixation limit layer diminishes as the Schmidt number Sc ascends, as displayed in Figure-15.

Because of the expansion in Sc, the mass diffusivity diminishes, bringing about a reduction in the thickness of the fixation limit layer. Figure 16 portrays the impact of substance definition boundary St_1 on the focus limit layer. It's significant that when St_1 ascents, the boundary layer of the fixation profile lessens. Figure-17 portrays the conduct of the substance response boundary Cr on focus profiles. The thickness of the fixation limit layer reduces as Cr grows. Figures 18, 19, and 20 show the effect of the pull boundary S on the speed, temperature, and fixation in the limit layer. The stream speed, temperature, and focus dissemination are seen to diminish as S increments

With various values of Jeffrey parameter λ_1, porosity parameter K, chemical stratification parameter St_1, Prandtl number Pr, magnetic parameter M, thermal stratification parameter St, Schmidt number Sc, heat source parameter Q_H, thermal radiation parameter R, Eckert number Ec, chemical reaction parameter Cr, and suction parameter S, Table 1 shows the deviation in skin friction coefficient, local Nusselt number, and local Sherwood number. The friction factor coefficient, the rate of heat and mass transfer coefficients all decrease as the values of λ_1, K, and M increase. We noted that as R, St, Q_H, and Ec increase, the heat transfer coefficient decreases, whereas Pr shows the opposite tendency. The Sherwood number is thought to increase with an increase in Sc and Cr, but decrease with an increase in St_1. The friction factor coefficient depreciates with an increase in S, although the rate of heat and mass transfer coefficients shows a contradicting tendency.

To approve the technique utilized in this review and to pass judgment on the exactness of the current investigation, correlation with accessible outcomes relating to the skin-friction coefficient $-\theta'(0)$ for $\lambda_1 = 0.0,\ M = 0.0,\ S = 0.0,\ R = 0.0,$ $Ec = 0.0,\ St_1 = 0.0,\ K = 0.0, Q_H = 0.0,\ Sc = 0.0,$ $Cr = 0.0$ are compared with the available results of N. L. Nazari *et al.* [37] and Nur Suhaida Aznidar ismail *et al.* [38] in Table-2 and they are found to be in good agreement.

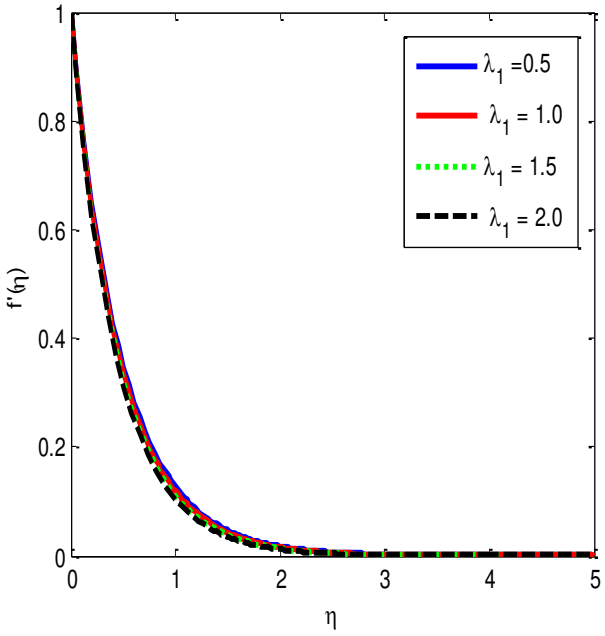

Figure-1. Velocity profiles for various upsides of λ_1.

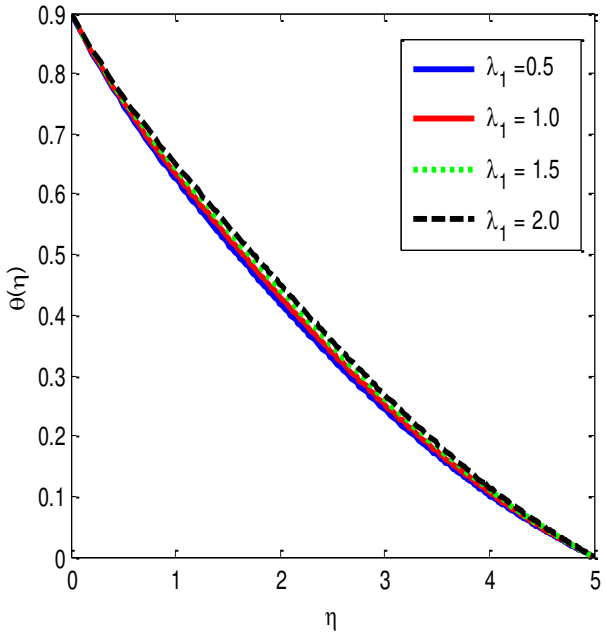

Figure-2. Temperature profiles for various upsides of λ_1.

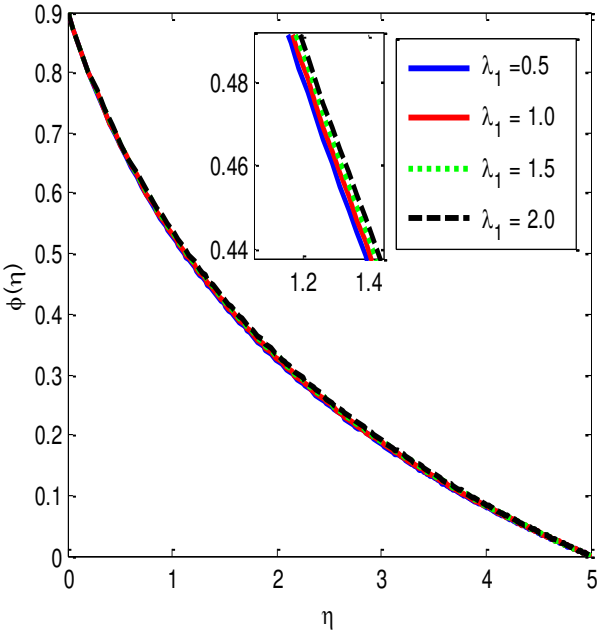

Figure-3. Concentration profiles for various upsides of λ_1.

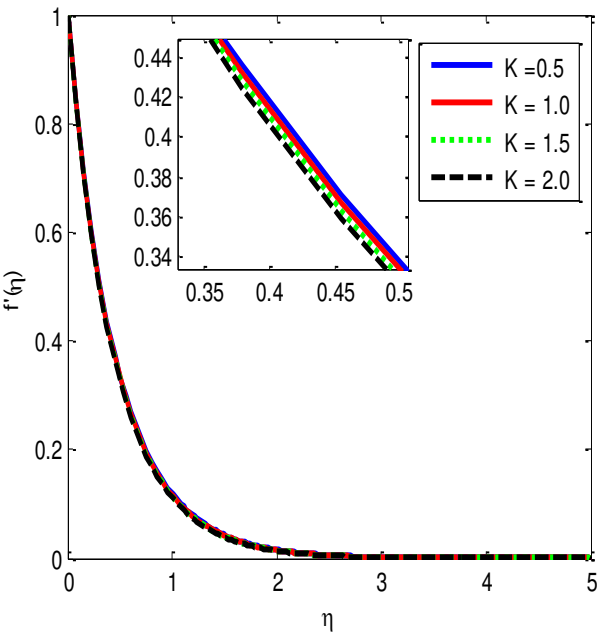

Figure-4. Velocity profiles for various upsides of K.

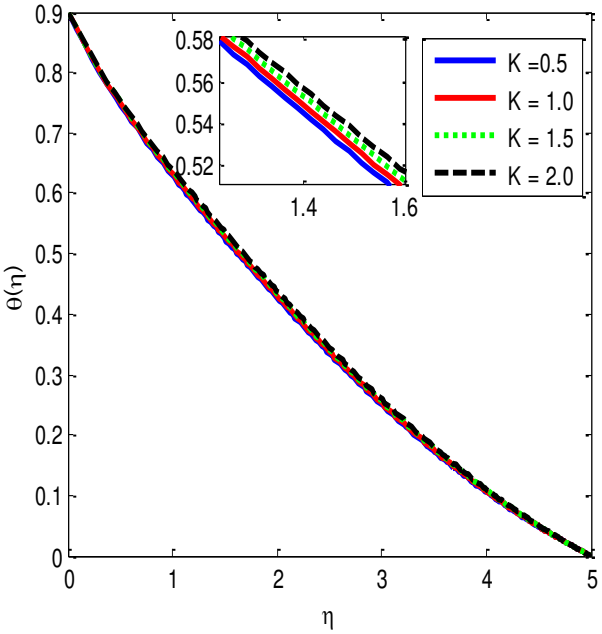

Figure 5. Temperature profiles for various upsides of K.

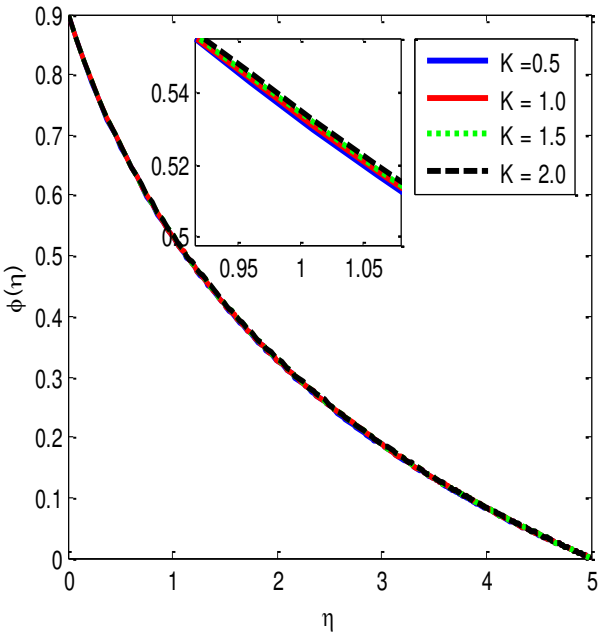

Figure-6. Concentration profiles for various upsides of K.

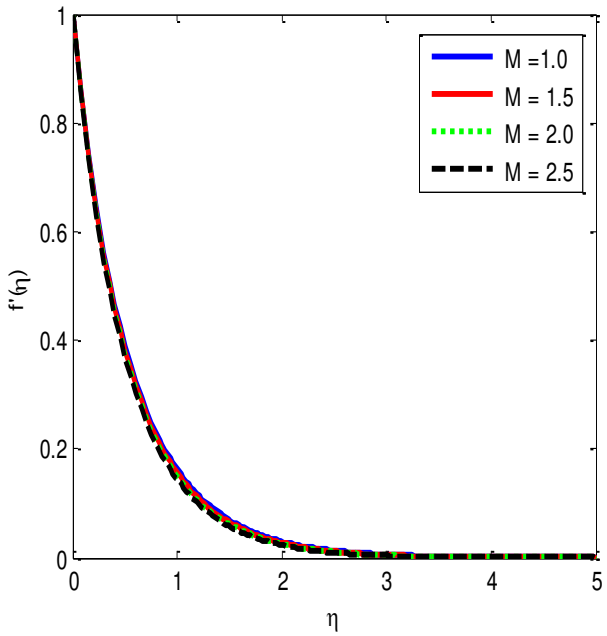

Figure-7. Velocity profiles for various upsides of M .

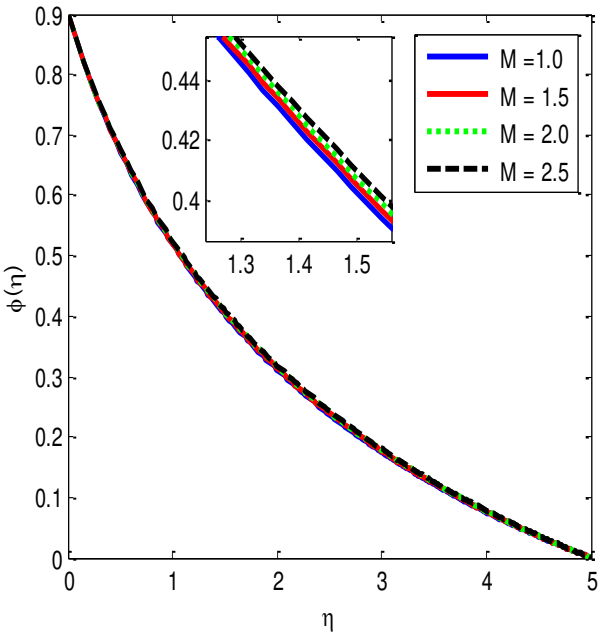

Figure-9. Concentration profiles for various upsides of M .

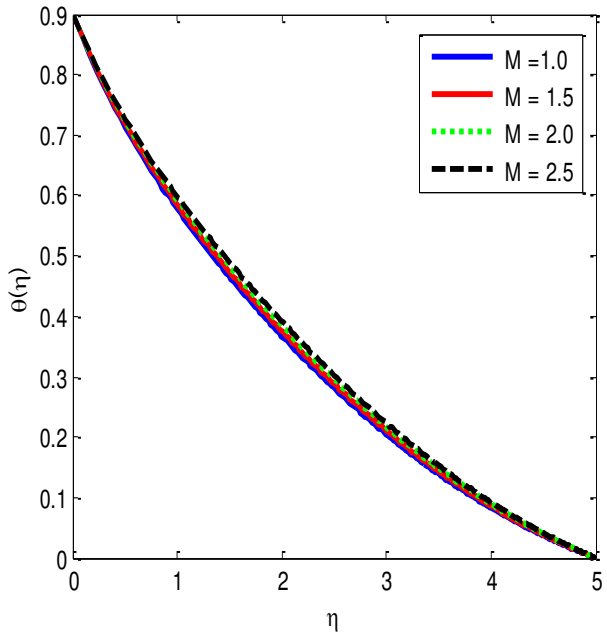

Figure-8. Temperature profiles for various upsides of M .

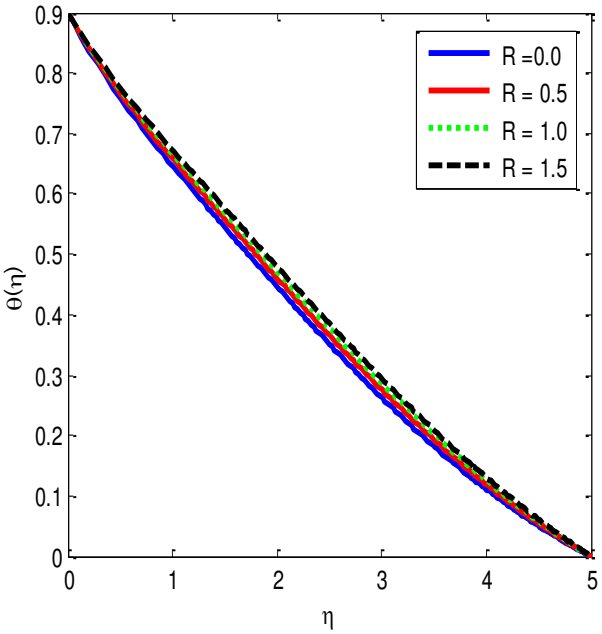

Figure-10. Temperature profiles for various upsides of R .

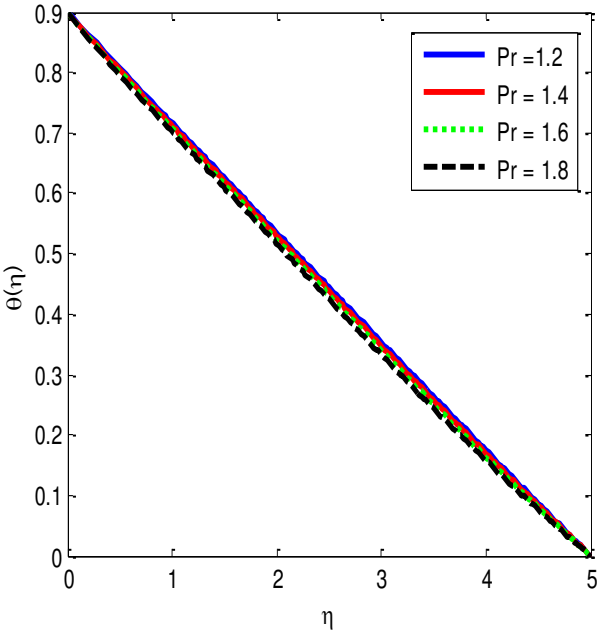

Figure-11. Temperature profiles for various upsides of $\Pr$.

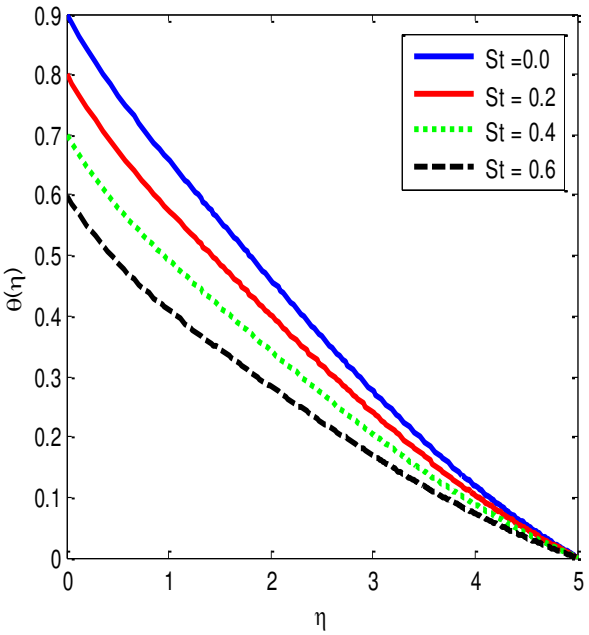

Figure-12. Temperature profiles for various upsides of St.

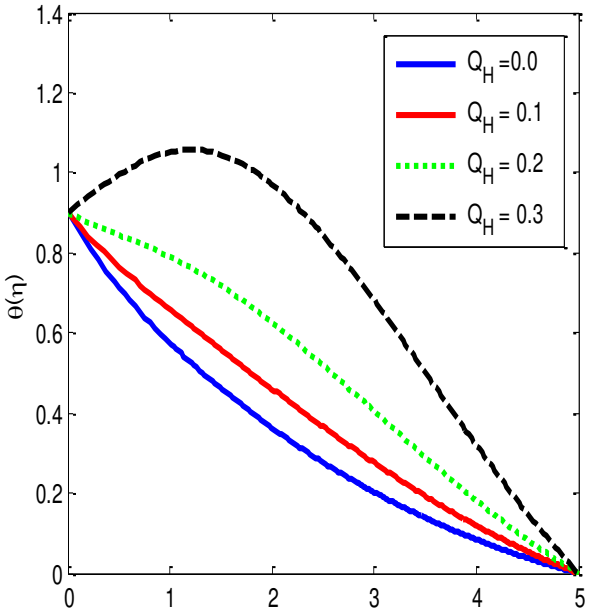

Figure-13. Temperature profiles for various upsides of Q_H.

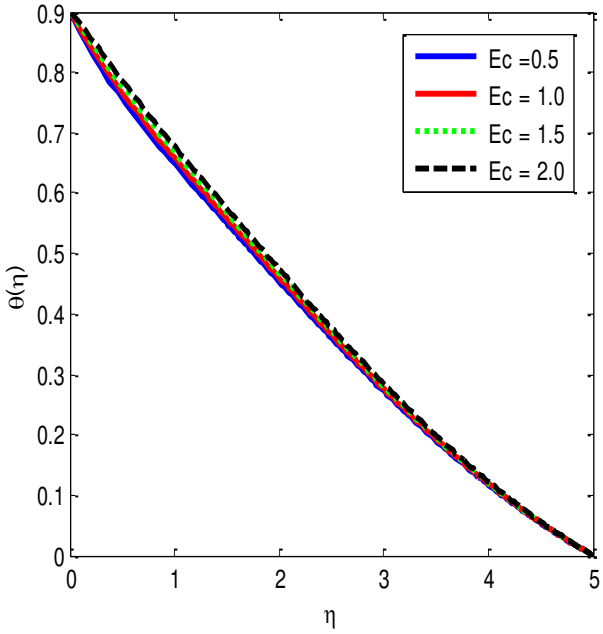

Figure-14. Temperature profiles for various upsides of Ec.

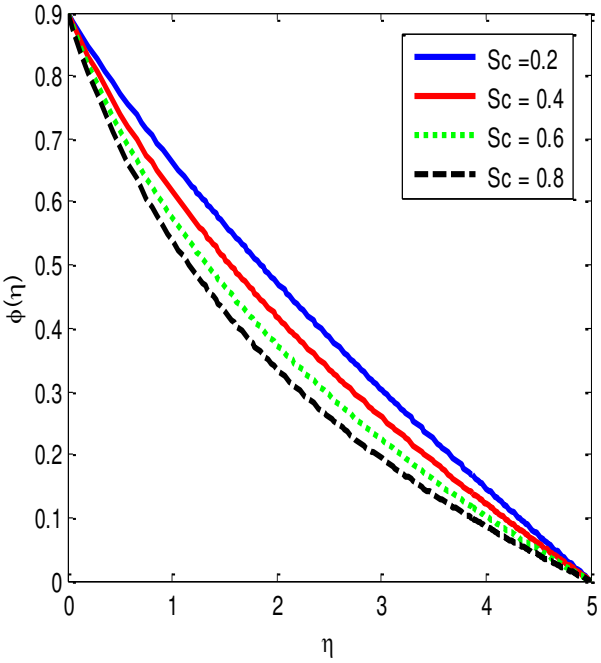

Figure-15. Concentration profiles for various upsides of Sc.

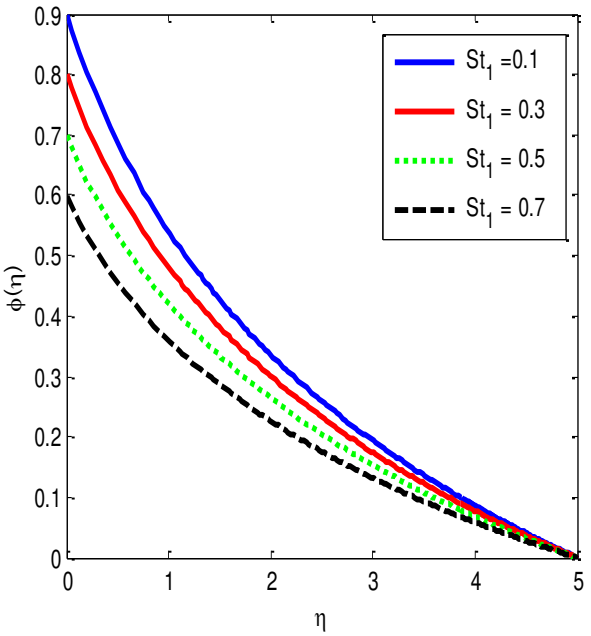

Figure-16. Concentration profiles for various upsides of St_1.

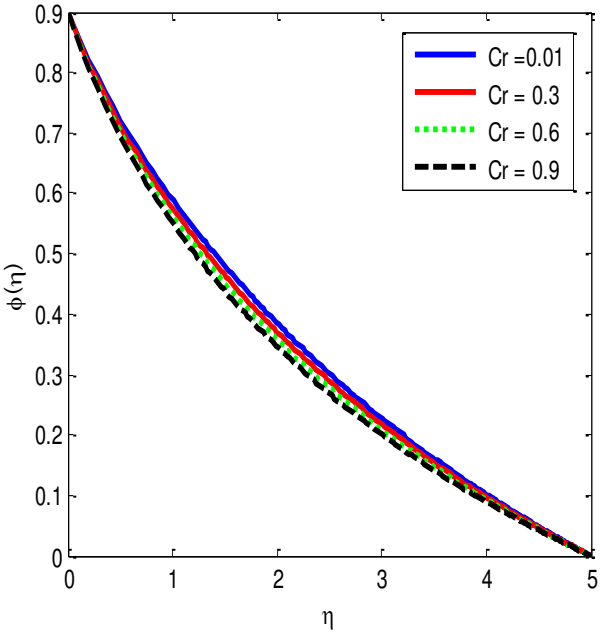

Figure-17. Concentration profiles for various upsides of Cr.

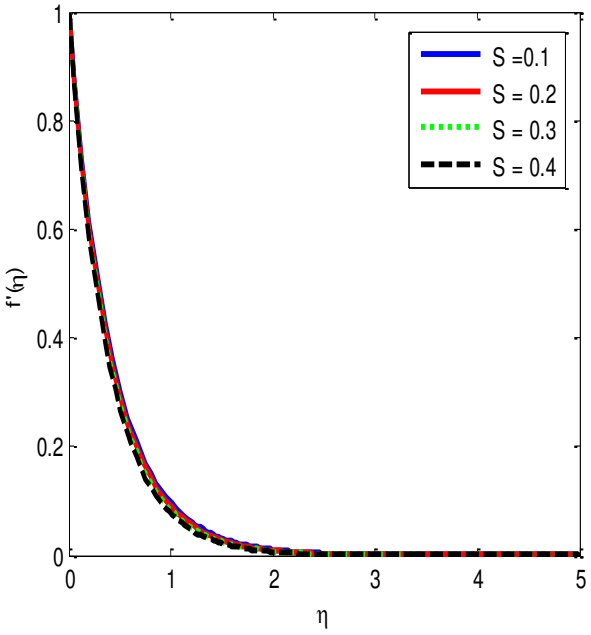

Figure-18. Velocity profiles for various upsides of S.

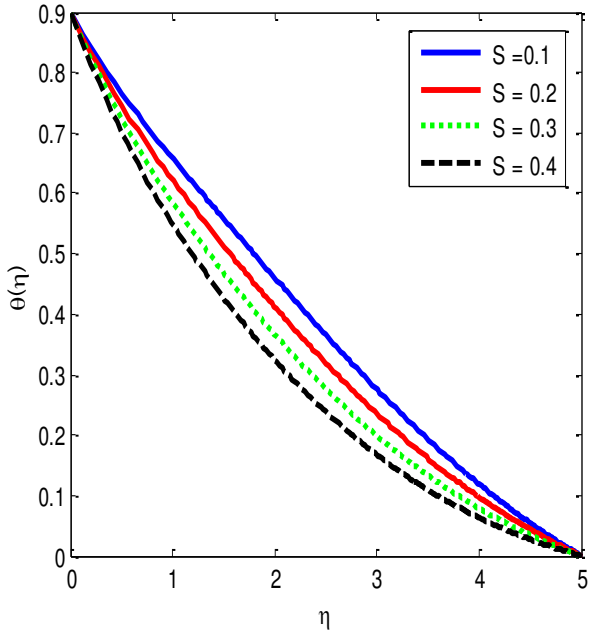

Figure-19. Temperature profiles for various upsides of S.

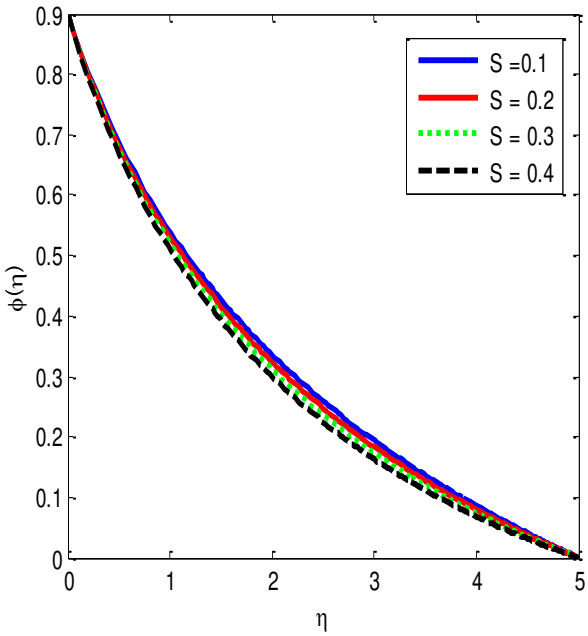

Figure-20. Concentration profiles for various upsides of S.

Table-1. Skin friction coefficient, Nusselt, Sherwood numbers for different values λ_1, K, M, R, Pr, St, Q_H, Ec, Sc, St_1, Cr, S.

λ_1	K	M	R	Pr	St	Q_H	Ec	Sc	St_1	Cr	S	$f''(0)$	$-\theta'(0)$	$-\phi'(0)$
0.5												**-2.469381**	**0.462363**	**0.596126**
1.0												-2.803657	0.444494	0.582314
1.5												-3.106088	0.428463	0.571537
	0.5											-2.362210	0.481716	0.601566
	1.0											-2.469381	0.462363	0.596126
	1.5											-2.571905	0.444559	0.591223
		1.0										-2.306671	0.492060	0.604521
		1.5										-2.469381	0.462363	0.596126
		2.0										-2.621604	0.436165	0.588945
			0.5									-2.017797	0.487024	0.621569
			1.0									-2.017797	0.431678	0.621569
			1.5									-2.017797	0.401534	0.621569
				1.2								-2.017797	0.602580	0.621569
				1.4								-2.017797	0.656152	0.621569
				1.6								-2.017797	0.710087	0.621569
					0.2							-2.017797	0.516510	0.621569
					0.4							-2.017797	0.450373	0.621569
					0.6							-2.017797	0.384240	0.621569
						0.1						-2.017797	0.609111	0.621569
						0.2						-2.017797	0.549579	0.621569
						0.3						-2.017797	0.484471	0.621569
							0.7					-2.017797	0.321695	0.621569
							1.0					-2.017797	0.184964	0.621569
							1.3					-2.017797	0.048233	0.621569
								0.2				-2.017797	0.549579	0.468894
								0.4				-2.017797	0.549579	0.621569
								0.6				-2.017797	0.549579	0.762369
									0.1			-2.017797	0.549579	0.621569
									0.3			-2.017797	0.549579	0.504957
									0.5			-2.017797	0.549579	0.397235
										0.3		-2.017797	0.549579	0.587878
										0.5		-2.017797	0.549579	0.621569
										0.7		-2.017797	0.549579	0.653584
											0.1	-2.017797	0.549579	0.621569
											0.2	-2.093875	0.581038	0.636695
											0.3	-2.172961	0.614440	0.652317

Table-2. Estimates of $-\theta'(0)$ with various upsides of Pr for $\lambda_1 = 0.0,\ M = 0.0,\ S = 0.0,\ R = 0.0,$ $St = 0.0, Ec = 0.0,\ St_1 = 0.0,\ K = 0.0,\ Q_H = 0.0,\ Sc = 0.0,\ Cr = 0.0$.

Pr	**N. L. Nazari *et al*. [37]**	**Nur Suhaida *et al*. [38]**	**Current study**
1.0	0.9547	0.9548	0.954854
2.0	1.4714	1.4715	1.471447
3.0	1.8691	1.8691	1.869064

5. CONCLUSIONS

The current review is a decent endeavor to check out the impacts of a second request substance response and twofold separation on MHD free convection Jeffrey course through a permeable medium over a dramatically broadening sheet. The MATLAB bvp4c programming was utilized to tackle the changed over conventional differential conditions mathematically. Our mathematical discoveries lead to the accompanying ends:

a) When the Jeffrey, magnetic, porosity, and suction parameters are increased, the dimensionless momentum decreases.

b) Raising the values of thermal stratification, Prandtl number and suction parameters the dimensionless temperature diminishes.

c) A rise in rate of reaction, Schmidt number, suction parameters and chemical stratification parameters diminishes the dimensionless concentration.

d) The friction factor coefficient, rate of heat transmission, and mass transfer coefficients decline as the levels of Jeffrey, porosity, and magnetic properties increase.

REFERENCES

[1] R. N. Jat, Santhosh Chaudhary. 2009. MHD flow and heat transfer over a stretching sheet, Appl. Math. Sci. 26(3): 1285-1294.

[2] M. Mustafa, T. Hayat, I. Pop, S. Asghar, S. Obaidat. 2011. Stagnation-point flow of a nanofluid towards a stretching sheet, Int. J. Heat Mass Tran. 54: 5588-5594.

[3] Samir Kumar Nandy, Tapas Ray Mahapatra. 2013. Effects of slip and heat eneration/absorption on MHD stagnation flow of nanofluid past a stretching/shrinking surface with convective boundary conditions. Int. J. Heat Mass Tran. 64:1091-1100.

[4] Iswar Chandra Mandal, Swati Mukhopadhyay. 2013. Heat transfer analysis for fluid flow over an exponentially stretching porous sheet with surface heat flux in a porous medium. Ain Shams Engineering Journal. 4: 103-110.

[5] I. Swain, S. R. Mishra, H. B. Pattanayak. 2015. Flow over exponentially stretching sheet through porous medium with heat source/sink. J. Eng. 7. Article ID 452592.

[6] E. M. A. Elbashbeshy. 2001. Heat transfer over an exponentially stretching continuous surface with suction. Arch. Mech. 53: 643-651.

[7] M. E. Ali. 1995. On thermal boundary layer on a power law stretched surface with suction or injection. Int. J. Heat Fluid Flow. 16: 280-290.

[8] K. Vajravelu. 2001. Viscous flow over a nonlinearly stretching sheet. Appl. Math. Comput. 124: 281-288.

[9] K. Vajravelu, J.R. Cannon. 2006. Fluid flow over a nonlinear stretching sheet, Appl. Math. Comput. 181: 609-618.

[10] S. K. Khan. 2006. Boundary layer viscoelastic fluid flow over an exponentially stretching sheet, Int. J. Appl. Mech. Eng. 11: 321-335.

[11] E. Sanjayanand, S. K. Khan. 2006. On heat and mass transfer in a visco-elastic boundary layer flow over an exponentially stretching sheet. Int. J. Therm. Sci. 45: 819-828.

[12] M. Sajid, T. Hayat. 2008. Influence of thermal radiation on the boundary layer flow due to an exponentially stretching sheet. Int. Commun. Heat Mass Transfer. 35: 347-356.

[13] S. Nadeen, N. S. Akbar, R. U. Haq, Z. H. Khan. 2013. Radiation effect on MHD stagnation point flow of nanofluid towards a stretching surface with convective boundary conditions. Chinese journal of Aeronautics. 26(6): 1389-1397.

[14] M. Ali, M. A. Alim, M. S. Alam. 2014. Heat transfer boundary layer flow past an inclined stretching sheet

in presence of magnetic field. International Journal of Advancements in Research & Technology (IJOART). 3(5): 34-40.

[15] M. K. Choudhary, S. Chaudhary, R. Sharma. 2015. Unsteady MHD flow and heat transfer over a stretching permeable surface with suction and injection. Procedia Engineering. 127: 703-710.

[16] M. A. Mohd Fauzi, A. S. Abd Aziz, Z. Md Ali, Heat and mass transfer in magnetohydrodynamics(MHD) flow over an exponentially stretching sheetin a thermally stratified medium. AIP Conference Proceedings. (1974) (2018) 020007.

[17] N. L. Nazari, A. S. Abd Aziz, V. Daniel David, Z. Md Ali. 2018. Heat and Mass Transfer of Magnetohydrodynamics (MHD) Boundary Layer Flow using Homotopy Analysis Method.Malaysian Journal of Industrial and applied mathematics. 34: 2018.

[18] Kharabela Swain, Sampada K. Parida and Gauranga C. Dash. 2019. Higher order chemical reaction on MHD nanofluid flow with slip boundary conditions: A numerical approach, Mathematical modeling of engineering. 6(2): 293-299.

[19] Anjana Matta, Nagaraju Gajjela. 2018. Order of chemical reaction and convective boundary condition effects on micropolar fluid flow over a stretching sheet. AIP advances, 8, Article ID 115212.

[20] Halima Usman, Ime Jimy Uwanta and Smaila Kanba Ahmad. 2016. Magnetohydrodynamics free convection flow with thermal radiation and chemical reaction effects in presence of variable suction. MATECWeb of Conferences. 64, Article ID 01002.

[21] K. Bhattacharyya. 2011. Effects of radiation and heat source/sink on unsteady MHD boundary layer flow and heat transfer over a shrinking sheet with suction/injection, Front. Chem. Sci. Eng. 5: 376-384.

[22] S. Mukhopadhyay. 2012. Slip effects on MHD boundary layer flow over an exponentially stretching sheet with suction/blowing and thermal radiation, Ain Shams Eng. J.

[23] S. Mukhopadhyay. 2011. Effects of slip on unsteady mixed convective flow and heat transfer past a porous stretching surface, Nuc. Eng. Design. 241: 2660-2665.

[24] S. Mukhopadhyay, MHD boundary layer flow and heat transfer over an exponentially stretching sheet embedded in a thermally stratified medium. Alexandria Engineering Journal, 52 (2013) 259-265.

[25] K. C. Sekhar. 2014. Boundary layer phenomena of MHD flow and heat and mass transfer over an exponentially stretching sheet embedded in thermally stratified medium. International Journal of Science, Engineering and Technology Research (IJSETR); 3(10): 2715-2721.

[26] K. Singh, M. Kumar. 2015. The effect of chemical reaction and double stratification on MHD free convection in a Micro Polar fluid with heat generation and Ohmic heating. Journal of Mechanical and Industrial Engineering (JJMIE). 9(4): 279-288.

[27] M. U. Ahammad, M. S. H. Mollah. 2011. Numerical study of MHD free convection flow and mass transfer over a stretching sheet considering Dofour and Soret effects in the presence of magnetic field. IJET-IJENS. 11(5): 4-11.

[28] J. Alinejad, S. Samarbakhsh. 2012. Viscous flow over nonlinearly stretching sheet with effects of viscous dissipation. Journal of Applied Mathematics. 2012: 10, Article ID 587834.

[29] O. Anwar B´eg, M. M. Rashidi, M. T. Rastegari, T. A. B´eg, S. S. Motsa, A. Halim. 2013. DTM-pade numerical simulation ´ of electrohydrodynamic ion drag medical pumps with electrical hartmann and electrical reynolds number effects. Journal of Advanced Biotechnology and Bioengineering. 1(2): 62-79.

[30] R. Cortell. 2014. MHD (magneto-hydrodynamic) flow and radiative nonlinear heat transfer of a viscoelastic fluid over a stretching sheet with heat generation/absorption, Energy. 74(1): 896-905.

[31] R. P. Sharma, M. Jain, S. R. Munjam, D. Kumar. 2017. Effects of ohmic dissipation and chemical reaction on MHD free convection flow through porous medium with thermal radiation. Journal of Ultra Scientist of Physical Sciences Section A. 29(08): 315-326.

[32] J. Pattnaik, C. Dash, L. Ojha. 2017. MHD falkner-skan flow through porous medium over permeable surface, Modelling, Measurement and Control B. 86(2): 380-395.

[33] S. J. Kim, K. Vafai. 1989. Analysis of natural convection about a vertical plate embedded in a porous medium. International Journal of Heat and Mass Transfer. 32(4): 665-677.

[34] S. J. Liao, I. Pop. 2004. Explicit analytic solution for similarity boundary layer equations. International Journal of Heat and Mass Transfer. 47(1): 75-85.

[35] R. S. Tripathy, G. C. Dash, S. R. Mishra, S. Baag. 2015. Chemical reaction effect on MHD free convective surface over a moving vertical plane through porous medium. Alexandria Engineering Journal. 52(3): 671-679.

[36] P. Nagur Meeraiah, B. Reddappa, A. Saila Kumari. 2020. Unsteady MHD boundary layer flow and heat transfer of a casson fluid past a stretching sheet. International Journal of Mechanical and Production Engineering Research and Development. 10(3): 12365-12374.

[37] N. L. Nazari, A. S. Abd Aziz, V. Daniel David, Z. Md Ali. 2018. Heat and Mass Transfer of Magnetohydrodynamics (MHD) Boundary Layer Flow using Homotopy Analysis Method. Malaysian Journal of Industrial and applied mathematics. 34.

[38] Nur Suhaida Aznidar Ismail, Ahmad Sukri Abd Aziz, Mohd Rijal Ilias, Siti Khuzaimah Soid. 2021. MHD Boundary Layer Flow in Double Stratification Medium, International Conference on Mathematical Sciences. Journal of Physics: Conference Series, IOP Publishing. 1770: 012045.